Electric Power Systems Research 185 (2020) 106349

Contents lists available at ScienceDirect

Electric Power Systems Research

journal homepage: www.elsevier.com/locate/epsr

Grid reduction for energy system analysis

Wolfgang Biener*, Klaus René Garcia Rosas

Fraunhofer Institute for Solar Energy Systems, Freiburg, Germany

ARTICLE INFO

Keywords:
Grid reduction
Equivalencing
Energy system analysis
Energy system modeling

ABSTRACT

Energy system models play an important role in evaluating potential pathways to a low-carbon energy system. Modeling the electrical grids within an energy system model raises the computational burden significantly. This is the reason why the grid is often reduced to a lower amount of nodes. While grid reduction is common in energy system models, the partitioning of the grid is mostly done manually. A grid reduction method is proposed that takes electrical parameters of the grid as well as other parameters, such as political borders or region-specific renewable potentials, into account. The proposed reduction method uses clustering based on electrical distance to identify regions with high electrical connectivity to minimize load flow deviations after the reduction. The method is compared against another state-of-the-art partitioning-based reduction method. The comparison shows that the partitioning plays an important role on the accuracy of line power flows when reducing grids for energy system analysis. An additional investigation is carried out on the ratio of recognized overloaded lines in the reduced grids. With respect to studied parameters, the proposed reduction method prevails. The findings can thus be used to more accurately reduce and represent electrical grids in energy system models.

1. Introduction

In the Paris Agreement, 196 countries pledged to limit temperature increase to a worst case of 2 °C, while pursuing an even further improvement of 1.5 °C of pre-industrial levels. Therefore, a transition to a low-carbon energy system is required to achieve these climate goals. Renewable power and heat generation, as well as the electrification of transportation will be the major contributors to a lower carbon-emitting future. As such, a robust and reliable energy system is required to facilitate the shift towards these new and emerging technologies. Energy system models are designed to find pathways to optimal combinations of technologies to determine a least-cost, reliable, and low carbon energy system.

Lopion et al. [15] and Ringkjøb et al. [17] scrutinize in a vast literature study recent trends in energy system modeling and their challenges in spatio-temporal variability. Lopion et al. [15] conclude that energy system models developed after 2010 are more flexible in spatial resolution. Spatial resolution enables the modeling of local weather conditions and local potential for renewable generation. These models are therefore able to calculate more localized results, and thus more accurately encompass local technologies. Lopion et al. [15] particularly highlight the trade-off in terms of computation time between temporal and spatial resolution. Spatial resolution of energy system models can be chosen according to various local criteria, such as political regions, zones of transmission system operators, population density, consumption of electrical energy, potential for the installation of photovoltaic or wind power plants. These criteria are well reasoned because they represent local differences that are highly important in energy systems and independent from transmission grid characteristics [21].

Regardless of the chosen spatial resolution, the grid has to be integrated into the energy system model to constrain the transport of power between chosen nodes or areas. Since costs for the extension of transmission capacity are high, grid constraints have a substantial impact on the location and choice of energy sources [12,13,16,19]. If spatial resolution does not fit to spatial distribution of the grid nodes, the grid has to be adapted to the energy system model.

Since the computational burden to integrate the original grid into large-scale energy system models is too high or would lead to an unacceptable loss of accuracy in other parts of the model, grid reduction is necessary to lower the number of nodes. Grid reduction methods for energy system models should satisfy three crucial criteria:

- Power flows on the remaining lines after reduction equal those from the original grid.
- Lines not taken into account after reduction are not overloaded.
- Quality of reduction is operating point independent.

Guaranteeing these characteristics ensures an accurate estimation of

* Corresponding author.
E-mail addresses: wolfgang.biener@ise.fraunhofer.de (W. Biener), klaus.rene.garcia.rosas@ise.fraunhofer.de (K.R. Garcia Rosas).

https://doi.org/10.1016/j.epsr.2020.106349
Received 27 August 2019; Received in revised form 25 February 2020; Accepted 24 March 2020
Available online 14 April 2020

overloaded lines, thus enabling an accurate optimization of transmission system expansion in long-term energy system studies. To our best knowledge, there are no methods available in literature which satisfy each of these three criteria. In this paper we propose a new approach of reducing electrical grids, which takes both grid characteristics as well as the previously mentioned spatial criteria into account. We compare the method to another partitioning-based reduction method and discuss the implications of grid reduction for energy system optimization, especially with respect to power flows and line overloads. In order to compare the power flows of the lines in the reduced grids with the ones in the original grid, we propose several quality indicators. Moreover, we scrutinize the detection rate for overloaded lines as well type I and type II errors. This helps to analyze the results of energy system models regarding line overloads.

The remainder of this paper is organized as follows. In Section 2 an overview on the state of the art regarding grid reduction literature is given. Section 3 describes how the state of the art is furthered by this publication. In Section 4, the used grid model, time steps and grid calculation methodology are defined. In Section 5, the proposed grid reduction methodology is described in detail. In Section 6, results of the proposed grid reduction methodology are presented and compared with a state of the art grid reduction methodology. Those results are discussed in Section 7. In Section 8 conclusions are drawn.

2. State of the art

There are two steps that are important for grid reduction. First, the grid needs to be partitioned into zones. Second, grid structures inside the zones are reduced. This section is divided into four parts. The first part lists grid reduction methodologies that are operating point dependent. Those methods are well known and widely studied due to their important role in power system stability analysis. They are mentioned here for the sake of completeness, even though they have no use for long-term planning. The second part explains operating point independent grid reduction methods. They are useful for long-term analysis but may lead to qualitative drawbacks as the partitioning of the grid plays a subordinate role. Grid partitioning methods in the subsection afterwards focus solely on the partitioning of the grid without considering grid reduction. However, they are introduced as our reduction method makes use of them. In the last subsection, grid reduction methods are presented which combine the partitioning and reduction process to improve the resulting grid representations for dynamic load cases.

Table 1 provides an overview of grid reduction methods which will be presented in this section.

2.1. Operating point dependent grid reduction methods

When using grid reduction methods like Ward [26] or REI (Radial, Equivalent, Independent) equivalents [8], predefined network parts will be replaced by reduced equivalents. In case of Ward equivalents, this is done by transferring the complex information including power injections and impedances of the part to be reduced to the boundary buses connected to this part. Power injections of the boundary buses are adapted accordingly and artificial lines added between them. Using bus admittance matrix transformations, the equivalent injections and impedances can be calculated. For REI equivalents, the network part to be reduced is transformed to an artificial generation and load node connected to each of the boundary buses. The calculation of equivalent nodal powers and impedances is also done by performing bus admittance matrix transformations. Both methods are designed for static networks with known complex bus powers. When using these methods, the reduced grid is highly dependent on the operating point. Dynamic energy production and demand would require several grids for different time steps to have high accuracy of system reactions to disturbances.

Table 1
Reduction methods characteristics.

Work	Partitioning	Reduction	OPI[a]
[26]	–	Ward	No
[8]	–	REI	No
[6]	–	Zonal PTDFs	No/Yes[b]
–	–	Bus-aggregation	Yes
[24]	K-means clustering using nodal PTDF differences	Zonal PTDFs	No/Yes[b]
[11]	K-means clustering using nodal geographic location, generation capacities and load	Bus-aggregation	Yes
Our method	Hierarchical clustering using electrical distance	Bus-aggregation	Yes

[a] Operating point independent
[b] Assuming DC load flow

2.2. Operating point independent grid reduction methods

Power Transfer Distribution Factors (PTDFs) represent line power changes relative to nodal power injections. Zonal PTDFs [6] are aggregated PTDFs describing the distribution of power flow when certain power is transferred from one zone into another. The accuracy of PTDFs are strongly dependent on the distance to the operating point for which they have been calculated, making recalculation necessary for dynamic load cases and grid reinforcement measures [14]. Nevertheless when the DC load flow model is assumed, PTDFs are suited for dynamic load cases. The DC load flow model is a linearized estimation of the AC load flow and can be used for grids with high voltages [23].

Current energy system models which are using grid reduction, for example [27,28] apply a simple bus-aggregation reduction. Buses lying inside of a region are assumed to be connected by a copper plate so that the subgrid inside of a region can be replaced by a single aggregated bus. Lines between two regions are kept unchanged. This reduction method is used especially for large-scale energy system analysis as it lowers the complexity. In contrast to the other presented reduction methods, the bus-aggregation method is operating point independent which is essential for energy system analysis with long time horizons. The bus-aggregation reduction is therefore used in this paper to reduce the grid.

2.3. Grid partitioning methods

While the previous subsection only describes the reduction of already partitioned networks, this section presents grid partitioning methodologies. Instead of partitioning the grid manually into parts, various clustering methods have been applied to partition the grid into zones including k-decomposition, k-means, hierarchical and spatial clustering [2,18]. The goal of all these clustering methods is to find a reasonable partition of the grid considering factors like average power flows, grid topology in terms of geographical distance or in terms of electrical distance. However, a reduction after the clustering is not covered in these papers.

Clustering based on electrical distance has been mainly used for structure recognition [2,25]. The impedance between two connected nodes is typically used as estimate of electrical distance. The effect of different voltage levels on electrical distance is taken into account by transforming all voltage levels to one common voltage level.

2.4. Grid reduction using partitioning

The partitioning of a grid plays a role on the reduction quality, especially when dynamic load cases are considered. In [24] and [11], the reduction covers both the clustering and the subsequent reduction. Svendsen [24] proposes a k-means clustering using nodal PTDF differences as a partitioning method. Zonal PTDFs are used to reduce the

grid. Hörsch and Brown [11] make use of initial univalent bus clustering combined with a subsequent k-means clustering to aggregate buses considering the buses' geographical positions, loads and generation capacities. Each cluster's subgrid is replaced by exactly one bus. Inter-cluster lines between the two identical clusters are replaced by a single equivalent line with equivalent impedances of parallel lines.

3. Research gap and objectives

The successful integration of grids into large-scale energy system models is highly dependent on the accurate reduction and adaptation of the grid, while maintaining operating point independence. As shown in the previous section, there is no reduction method which includes the electrical grid already at the partitioning phase. Considering the electrical grid in the partitioning phase might improve the load flow behavior of grid reduction methods. Therefore we propose a new electrical distance based reduction method (*ED-reduction*) which considers grid characteristics during the partitioning and reduction process. The applied density-based hierarchical clustering method divides the grid into zones with high intra-cluster connections and sparse inter-cluster connections in terms of electrical distance. Afterwards, each zone's subgrid is replaced by a single node. The resulting reduced grid is operating point independent. To survey the performance of this method, the method is compared to an adapted version of the grid reduction used in Hörsch and Brown [11], further referred to as *PyPSA-reduction*. The PyPSA-reduction is chosen as comparison method since it is the only well described reduction methodology that uses a similar reduction technique after the partitioning. It is essential to quantify the quality of reduced grid representation, so that the effect of grid reduction can be determined. This paper proposes quality indicators and applies them to the ED-reduction method, and the PyPSA method. The quality indicators particularly focus on quantifying the accurate detection of overloaded lines.

4. Grid modeling and load cases

The investigations on the quality of reduced grids use the ELMOD-DE grid model, created in Egerer et al. [9], as an original grid which represents the German transmission grid with line voltages of 220 kV and 380 kV. The model consists of 416 nodes and 657 lines which are entirely inside Germany. Today's conventional generation capacities, potential generation and demand loads at the nodes are determined regionally (NUTS3) and divided equally to corresponding inside-lying nodes. Generation capacities are obtained from the power plant list of the German Bundesnetzagentur [5]. They are aggregated into NUTS3 regions and divided by type. Loads are determined by the hourly load profile for Germany published by the ENTSOE [10]. The cost-minimal unit commitment of power plants for each NUTS3-level is optimized by the ENTIGRIS energy system optimizer [22] for a decentralized renewable energy system in the year 2050. This assures that grid reduction methodologies are tested with a renewable decentralized energy system. As all extreme grid loads are taken into account by the defined load cases, all other possible load and generation distributions would result in lower grid loads. Hence the choice of load cases guarantees robustness towards changing load and generation distributions.

15 exemplary load cases listed in Table 2 are used for comparing the load flow behavior in different grids. The load cases are defined by combinations of average and extreme cases with respect to spatial load and generation distribution for a year. Specifically, these are combinations of mean, median, maximal and minimal loads, large-scale photovoltaic generation (PV large), rooftop photovoltaic (PV roof) and wind generation. Due to the high amount of calculated grid nodes, time steps taken into account to calculate this scenario were only those 15. This means the scenario is not valid to draw a conclusion on the resulting energy system, but it has a good chance to contain all grid dimensioning time steps. This means if the grid is not overloaded for each of these time steps, it should not be overloaded during the rest of the year.

Table 2
Load cases.

#	Characteristic	Time step
1	mean load	02–15 12:00
2	min PV large / min PV roof	03–08 04:00
3	max PV roof	04–18 13:00
4	max PV large	04–19 13:00
5	mean PV large	05–22 13:00
6	min load	05–25 05:00
7	median PV large	06–29 11:00
8	median load	07–11 13:00
9	median PV roof	07–29 17:00
10	mean wind	07–30 20:00
11	min wind	09–17 20:00
12	mean PV roof	11–21 09:00
13	max load	11–24 18:00
14	median wind	12-05 21:00
15	max wind	12-10 14:00

For calculating AC power flows the program PyPSA [3] was used. Due to a lack of reactive power control information within the transmission grid, each node was modeled as a PV-node. This means that reactive power consumption at each node is used to control voltage, while maintaining a fixed active power consumption and production. Modelling every node as PV node is allowable since in the future energy system there is generation at every node which is able to control voltage by reactive power provision.

5. Methodology of the grid reduction

The ED-reduction consists of two main steps: a clustering of grid nodes based on electrical distance, and the subsequent adjustment of the grid to the given clusters. The clustering is based on the assumption of *primarily nearby power balancing*. That means that independent of the operating point, nodes are clustered in a way that power balances of nodes inside the same cluster primarily balance themselves before they affect the power balances of nodes which lie outside of the cluster. In this way, power balances of the same cluster can be aggregated without affecting the load flow behavior of the grid significantly. In Section 5.1 the clustering procedure of the grid nodes based on electrical distance is presented. The subsequent step, which consists of combining grid nodes in the same cluster and replacing them by one node, is described in Section 5.2. Section 5.3 shows how additional local parameters can be integrated into the clustering procedure, whereas Section 5.4 shows how constraints can be integrated into the clustering procedure.

5.1. Grid clustering

In the first step, the grid is clustered using a density-based graph clustering. Graph nodes represent the grid nodes and graph edges correspond to the grid lines. As the clustering is done for a high voltage grid, the DC load flow model is assumed. Electrical distance is therefore described by reactances instead of impedances. Reactances are additionally normalized by transforming all voltage levels at one common voltage level. As most rating measures for graph clusterings are based on similarity weights. The weight is represented by the inverted reactance. The weight w between two connected nodes $i \in N$ and $j \in N$ is therefore defined by $w_{ij} = \frac{1}{x_{ij}}$.

At the beginning, each node is a separate cluster. As initial clustering each node with only one neighboring node is clustered together with its neighbor. This process is repeated, treating nodes of the same cluster as single aggregated nodes, until each node has at least two

neighbors.[1]

After the initial clustering procedure, agglomerative clustering is used to iteratively aggregate pairs of clusters which produce the highest rating increase using *modularity* [7] as a rating measure. For a graph $G = (V, E)$ with vertices V and edges E and a set of clusters C, modularity Q is defined as

$$Q(G, C) = \frac{1}{2|E|} \sum_{v,w \in V} (A_{vw} - \frac{d_v d_w}{2|E|}) \delta(c(v), c(w)) \quad (1)$$

For a weighted graph, $|E|$ is the sum of all edge weights in the graph. A is the graph's weighted adjacency matrix with entries defined by $A_{ij} = w_{ij}$ if there is an edge between i and j and $A_{ij} = 0$ if not. d_k describes the weighted degree of node k which equals the sum of k's incident edge weights. $c(k) \in C$ is the cluster to which node k belongs. $\delta(x, y)$ is a boolean function with $\delta(x, y) = 1$ if $x = y$ and $\delta(x, y) = 0$ if $x \neq y$. Modularity sums up the actual fraction of the edges minus the expected fraction of edges inside of each cluster if edges were distributed randomly in the graph. Modularity reaches a high value if a graph has strong intra-cluster and sparse inter-cluster connections. During each clustering step, the two clusters which produce the highest modularity increase will be aggregated. Using this clustering procedure, it is possible to specify the number of desired clusters and stop when this number is reached. Alternatively, the algorithm can run until the end. During the run, all interim cluster configurations will be saved. Finally, the number of clusters which produce the maximal modularity can be chosen.

5.2. Grid adjustment

After the clustering, each cluster's subgrid is replaced by a single node as shown in Fig. 1. This replacement is also known as the copper plate approach as it is equivalent to all nodes inside of a cluster being connected to a lossless copper plate. In the end, intra-cluster lines will be removed and inter-cluster lines kept. Reactances and geographical line lengths for inter-cluster lines stay the same. The copper plate approach is broadly used for grid reductions in energy system analysis and performed very well compared to other adjustment methods [1].

5.3. Multiple parameters

The agglomerative nature of the clustering allows the weights between nodes to not only be represented by electrical distance, but also by other parameters such as power generation type, generation capacities, potential for the installation of renewable energies, demand, line capacities, overload potential and all other manner of quantifiable parameters which can be attributed to a node, region or line. Other parameters might be present which represent relationships between nodes not directly connected together. As such, a complete graph might be considered as a rating graph from which modularity can be calculated. When clustering a set for multiple variables, the weight of the variables has to be chosen. Normalization and standardization equalize variables influence on the results. In the next step weights of variables can be adapted to the desired objectives.

In a complete graph, every pair of distinct nodes is connected by an edge. As electrical distance is defined only between connected nodes, non-directly connected nodes will get a value of 0 as similarity edge weight in the complete rating graph.[2] One has to keep in mind that making weights heavily dependent on other parameters might disturb the functionality of the reduction. The reason is that the reduction method is founded on graph clustering finding densely connected node groups in terms of electrical distance. Alternatively the modularity rating function based on electrical distance can be combined with other score functions which evaluate other quantifiable parameters to produce an overall score function. In the latter case the evaluation of the grid structure and grid node parameters are independent from each other but require additional runtime to calculate the supplementary scores.

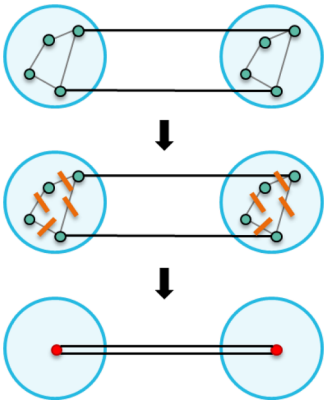

Fig. 1. Principle of copper plate methodology: Subgrid of each cluster is replaced by a single node. Line lengths of inter-regional lines stay the same.

5.4. Constraint-Integration

The agglomerative clustering procedure has two crucial properties allowing for integrating constraint checking during the clustering process. The first is the "step forward" property stating that nodes which have been assigned to the same cluster will never be separated in the remaining process. Sometimes it is desirable that nodes inside of certain areas should belong to the same clusters. This can be fulfilled by initially clustering the desired nodes and proceeding with the standard clustering procedure. For each area, the inside-lying nodes will always belong to the same cluster after the clustering process. The second advantage comes from the "step-by-step" functionality: Before each step (which involves merging two clusters) all temporary possible cluster combinations can be checked against defined constraints. In this way, for example, equal size constraints can be additionally integrated by adding penalties if cluster sizes differ too much.

6. Results

The ED-reduction methodology is compared to the PyPSA-reduction used in Hörsch and Brown [11].[3] The weights for the ED-reduction depend only on the electrical distance. No further parameters and no constraints on merging are used. All results are calculated using the grid and the 15 load cases described in Section 4. For better scaling and comparison between the resulting reduced grids, usage rates of lines are considered instead of power flows. A line usage rate equals 100% if 70% of its capacity has been reached to fulfill the n-1 security criterion [4]. Exceeding 100% of a line usage rate is considered as an indicator for reinforcement. The increase of complexity of an energy system

[1] In the trivial case where a graph component has no circles, exactly one node with no neighbors will be left afterwards.

[2] If weights are still dependent only on electrical distance and not on other parameters, using the complete rating graph will produce the same modularity ratings as if the original grid graph had been used. This is because the adjacency matrix A is the same in both cases no matter which method is used: the grid graph with no edges between non-connected nodes or the complete rating graph with weights of 0 between non-connected nodes.

[3] However instead of advising conventional power plant data and power distribution using Voronoi cells to grid nodes, which is originally done in Hörsch and Brown [11], power plant data and loads are regionally given and equally distributed to the corresponding inside-lying nodes.

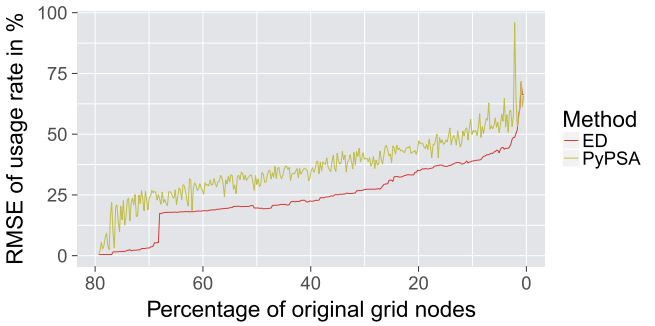

Fig. 2. RMSE of line usage rates for different reduction degrees and the two reduction methods.

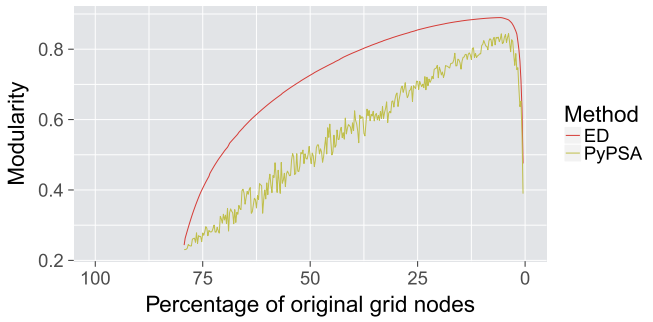

Fig. 3. Clustering modularity of two discussed methods using electrical distance as graph weights at different reduction degrees.

model due to integrating a grid can be inferred from the number of nodes. Therefore it is reasonable to define the reduction degree as a ratio of the number of nodes in the reduced grid compared to that in the original grid. In the following, the expression *% of the original nodes / size* will be used which is defined as the percentage of the number of nodes in the reduced grid compared to the number of nodes in the original grid.

6.1. General quality

To get a initial measure of general quality and significance of other statistical measures the *root-mean-square error* (*RMSE*) is calculated for both reduction methods. The RMSE is defined as

$$RMSE = \sqrt{\frac{\sum_{l\in L, t\in T} (U_{red}(l,\, t) - U_{org}(l,\, t))^2}{|T||L|}} \tag{2}$$

where T are all load cases defined in Table 2. L are the inter-cluster lines which will be kept in the reduced grid. $U_{red}(l,\, t)$ and $U_{org}(l,\, t)$ are the usage rates of line $l \in L$ and load case $t \in T$ signed by their flow direction in the reduced and the original case respectively. In each case the RMSE is calculated for all line usages and all load cases.

Fig. 2 shows the RMSE of line usage rates for the two reduction methods and all possible degrees of reduction in comparison to the corresponding usage rates of the original grid. For both reduction methods the grid could be scaled down to 80% of the original nodes without affecting the load flows of the reduced grid lines. This is because of the initial allocation of nodes which only have one neighbor, like described in Section 5.1. As the load needs to pass the original neighbors to reach the reduced nodes, aggregating the nodal loads and removing the corresponding lines will not affect the remaining part. The ED-reduction generally outperforms the PyPSA-reduction (neglecting really high reduction degrees, where are good grid representation is not expected), particularly in less extensive reduction in the range from 80% to 68% of the original nodes. The ED-method reaches a RMSE of 5% and the PyPSA-method a RMSE of 23% at 68% reduction degree.

6.2. Modularity as a measure for load flow behavior

The ED-reduction algorithm uses modularity as defined in (1) as a rating measure and tries in each step to combine pairs of clusters which will produce the highest modularity increase. The modularity rating is only dependent on the graph and the clustering. The grid adjustment after the clustering does not influence the rating. To evaluate the significance of modularity on load flow behavior, the modularity is shown in Fig. 3 for all reduction degrees of the ED- and PyPSA-method. For both cases, the modularity is calculated using the electrical distances as edge weights of the graph. In general, modularity is increasing for both reduction methods from 80% on until about 5% of the original nodes. With the PyPSA-method, modularity has the tendency to increase by a constant value for this range. The modularity using the ED-method initially strongly increases, with the slope constantly decreasing until the maximal modularity value where 5% of the original nodes are preserved. Further intensifying the reduction after 5% of the original size, the modularity drops suddenly for both methods.

Comparing the modularity of both methods for specific reduction degrees, it largely correlates with the corresponding RMSE results in Section 6.1. While having an almost similar modularity and RMSE at 80% of the original size, the modularity and RMSE difference between the two methods generally increases until about 48% of original size followed by a general decrease until the largest possible reduction.

6.3. Specific analysis on grid reinforcement

Costs for grid reinforcement play an important role in energy system analysis. In order to show how grid reduction influences the prediction of grid reinforcement measures, a statistical evaluation is conducted, followed by a comparison of detected line overloads for a further reduction to 30% of the original size. The 30% reduction degree is chosen as it is a conceivably realistic value being used in an energy system analysis. Using the ED-reduction, 273 lines of 657 original lines remain. Using the PyPSA-reduction, 387 lines remain.

The results of the statistical evaluation can be seen in Fig. 4. Three error measures are taken into account to analyze the extent at which line usage rate differences impact the prediction of grid reinforcement measures. The comparison is done between inter-cluster lines of the reduced grids and the corresponding lines of the original grid. Data for the box plot was obtained from a comparison of the lines across all 15 load cases.

The first measure is the *maximal error*:

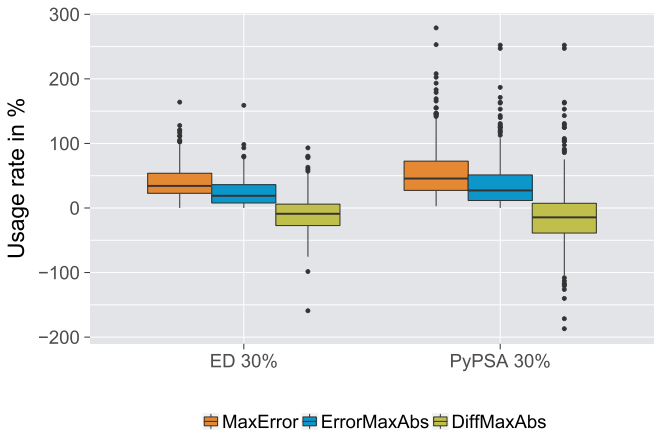

Fig. 4. Comparison of the ED- and PyPSA-reduction to 30% of the original grid nodes. MaxError: Maximal Error between usages. ErrorMaxAbs: Error of the maximal absolute values. DiffMaxAbs: Difference of maximal absolute values.

$$MaxError(l) = \max_{t \in T} |U_{red}(l, t) - U_{org}(l, t)| \quad (3)$$

It shows for each line the maximal usage error between the reduced and the original grid for all load cases. This measure shows the maximum error that happens in one of the load cases. The ED-reduction outperforms the PyPSA-method. The median amounts to 34% for the ED-reduction and 46% for the PyPSA-reduction. However, several lines exist for both methods which have high expected maximal errors reaching values up to 164% for the ED-method and up to 279% for the PyPSA-method.

The second measure is the *error of maximal absolute values*:

$$ErrorMaxAbs(l) = |\max_{t \in T} |U_{red}(l, t)| - \max_{t \in T} |U_{org}(l, t)|| \quad (4)$$

The ErrorMaxAbs calculates for each line the error between the maximal absolute usage rate value of all load cases in the reduced case and the maximal absolute value of all load cases in the reference case. This measure can be used as expected error of the maximal absolute usages. It is essential for detecting to what extent the reduced grid can be used as an indicator for grid reinforcement as the grid reinforcement depends on the highest absolute usage rate value. Looking at the results, the ED-reduction again with a median error of 19% performs better compared with the PyPSA-reduction with a median of 27%. The highest error value amounts to 159% for the ED-reduction and 252% for the PyPSA-reduction.

The third measure is the *difference of maximal absolute values*):

$$DiffMaxAbs(l) = \max_{t \in T} |U_{red}(l, t)| - \max_{t \in T} |U_{org}(l, t)| \quad (5)$$

The DiffMaxAbs differs from the ErrorMaxAbs showing if a line usage is over- or under-estimated. The DiffMaxAbs subtracts from each line's maximal absolute usage rate value of all load cases in the reduced case, the corresponding value of the reference case. A positive value indicates an overestimation of the maximal line usage rate in the reduced case. This leads to the detection of a line as overloaded in the reduced case although it is not overloaded in the original case (*false positive*). A negative value indicates an underestimation of the maximal line usage rate in the reduced case. In this case, a line may not be detected as overloaded although it is overloaded in the original grid (*false negative*). This error is crucial for energy system analysis as decisions for line upgrades are directly made as a result of overloaded lines. The ED-reduction again performs better than the PyPSA-method, when comparing DiffMaxAbs. Slightly more maximal absolute line usage rates are underestimated in the reduced grids. Nevertheless, there is no general tendency for both methods whether the maximal absolute line usage rates are strongly under- or overestimated. For the ED-reduction, the DiffMaxAbs values range from −159% to 93%, whereas for the PyPSA-reduction, the DiffMaxAbs values are between −186% and 252%. A specific analysis of the accuracy of overload detection is done in the next subsection.

6.4. Analysis of overload detection

Fig. 5 shows all grid lines in terms of overload detection for the ED-reduction to 30% of the original size. Falsely detected non-overloaded and overloaded lines (false negative and false positive) are visualized by thick red solid and dotted lines. Correctly detected non-overloaded (*true negative*) and overloaded lines (*true positive*) are visualized by solid and dotted lines with medium thickness and green color. Thin gray solid lines are not overloaded in the original grid but not present in the reduced grid (*NA negative*), while thin grey dotted lines are overloaded in the original but likewise ignored in the reduced grid (*NA positive*). One can see that, due to the initial clustering, lines between two nodes from which one node has only a single neighbor have been iteratively removed in the reduced grid.

Line counts for different classifications of overload detection and various reduction degrees are displayed in Table 3. Table 3a shows the detailed number of lines for each classification. Table 3b summarizes the correctly and incorrectly detected number of lines when not considering the removed lines after reduction in both the reduced and the original grid. Table 3c additionally takes the NA negative values as correctly detected and the NA positive values as falsely detected into account.

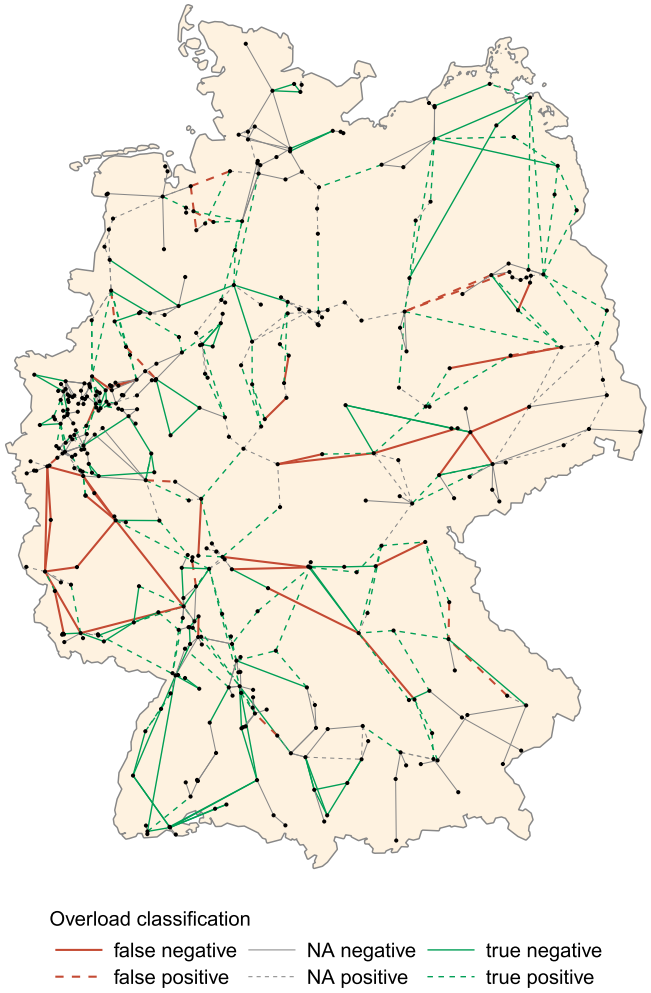

Fig. 5. Detected line overloads and non-overloads in the reduced grid compared to the ones in the original grid for the ED-reduction to 30% of original grid nodes.

Table 3
Line overload detection: number of lines.

Reduction ▷	ED			PyPSA		
▽ Classification	50%	30%	20%	50%	30%	20%
(a) Classification						
false negative	34	35	35	50	63	67
false positive	11	14	12	19	27	25
true negative	158	91	65	196	142	102
true positive	195	133	99	207	146	110
NA negative	185	249	277	139	185	227
NA positive	74	135	169	46	94	126
(b) Summary excluding NA						
True detect	353	224	164	403	288	212
False detect	45	49	47	69	90	92
Accuracy	89%	82%	77%	85%	76%	70%
(c) Summary including NA						
True detect	538	473	441	542	473	439
False detect	119	184	216	115	184	218
Accuracy	82%	72%	67%	82%	72%	67%

Table 4
Accumulated line lengths of reduced and original grid.

(a) Total lengths

Reduction ▷	ED			PyPSA		
▽ Total	50%	30%	20%	50%	30%	20%
Reduced in km	21,881	17,204	14,386	23,065	20,752	18,026
Original in km	26,609	26,609	26,609	26,609	26,609	26,609
Reduced/Original	82%	65%	54%	87%	78%	68%

(b) Overloaded lengths

Reduction ▷	ED			PyPSA		
▽ Overloaded	50%	30%	20%	50%	30%	20%
Reduced in km	11,314	8369	6679	11,076	8745	6795
Original excl. NA in km	13,049	10,840	9077	13,510	12,297	11,036
Original incl. NA in km	14,471	14,471	14,471	14,471	14,471	14,471
Reduced/Original excl. NA	86%	77%	74%	81%	71%	62%
Reduced/Original incl. NA	78%	58%	46%	76%	60%	47%

Not considering the removed lines after reduction (Table 3b), 353 correctly and 45 incorrectly detected lines have been determined for the ED-reduction to 50% of original grid nodes. For this reduction degree, the overload detection of the ED-method is still successful for 89% of the lines while the PyPSA-method is successful for 85% of the lines. Looking at the lines which have been removed due to the reduction (Table 3a), 74 additional line overloads have not been observed using the ED-method while for the PyPSA-method only 46 additional line overloads were missing. Taking the NA negative values as correctly detected and the NA positive values as falsely detected into account (Table 3c), both methods are successful for 82% of the lines.

Intensifying the reduction to 30% of original grid nodes, the accuracy amounts to 82% for the ED-method and 76% for the PyPSA-method when not considering NA values. Considering NA values like before, both methods reach an accuracy of 72%.

For a further reduction to 20% of original grid nodes, 77% and 70% accuracy could be reached when ignoring NA values for the ED- and PyPSA-method respectively. 67% accuracy could be reached for both methods when considering NA values. Although accuracy values are still high, intensifying the reduction also leads to an increased number of ignored overloaded lines for both reduction methods.

The accumulated line lengths for the detailed classification are available in Appendix A. The corresponding summaries are displayed in Table 4. Table 4a shows the total line lengths of the reduced and original grid and their ratio for different reduction methods and degrees. Table 4b shows the line lengths of the overloaded lines in the reduced and the original grids and their ratio. For the original grid, again, both variants excluding the removed lines and including the removed overloaded lines are considered.

In the original grid, 14,471 km of accumulated line length from a total of 26,609 km was detected as overloaded (*Original incl. NA*). When only observing the remaining lines of the grid reduced by the 50%-ED-reduction, the overloaded lines have a total length of 13,049 km in the original grid (*Original excl. NA)* and a total length of 11,314 km in the reduced grid (*Reduced*) so that 86% of the original overloaded line length has been detected (*Reduced/Original excl. NA*). Reducing the grid to 50% of the original nodes, the accumulated overloaded line length is closer to the original length when using the ED-reduction, resulting in a 14% detection rate deviation than using the PyPSA-reduction, resulting in a 19% deviation. This also holds for the 30%- and 20%-reduction reaching detection rates of 77% and 74% for the ED-method and 71% and 62% for the PyPSA-method respectively. Interestingly, the detection rate decreases for both methods with greater the reduction, even though in each case exactly the same lines are compared between the reference and the reduced grid.

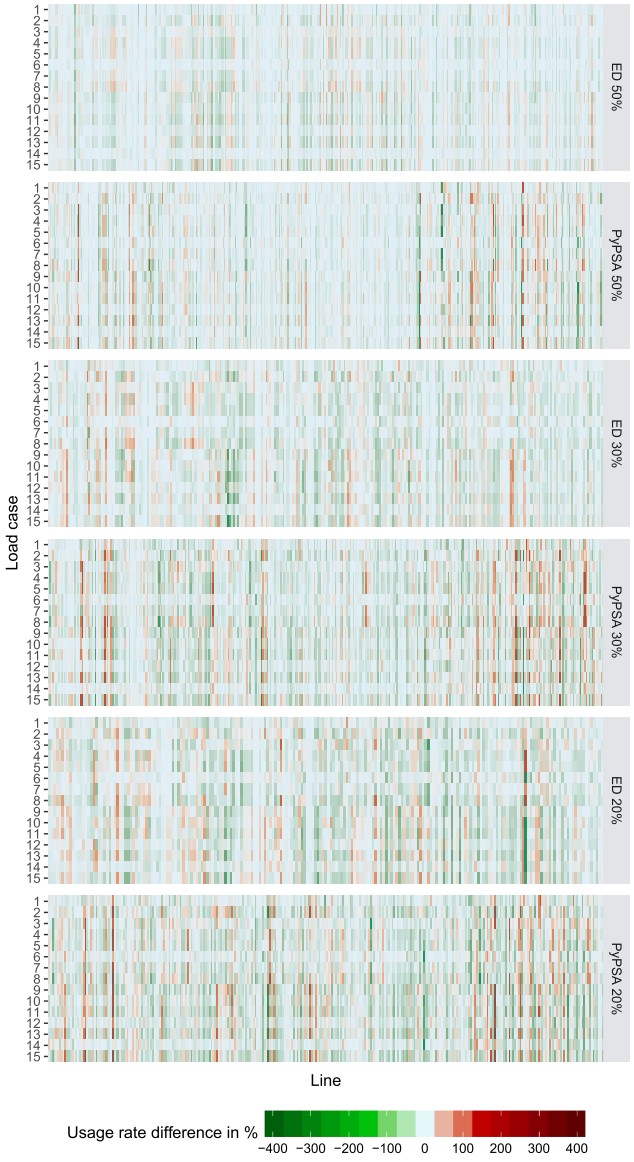

Fig. 6. Usage rate differences of all lines and load cases for the ED- and PyPSA-reduction to 50%, 30% and 20% of original grid nodes.

6.5. Specific analysis of load flow differences

A detailed comparison on load flow differences is done for a grid reduction to 50%, 30% and 20% of the original size.

Fig. 6 shows a heat map where the usage rate differences between the reduced and the original grid are visualized for each combination of lines, which are still present in the reduced grid and each of the 15 load cases. The x-axis shows the remaining lines for each reduction method. The lines on the x-axis do not correlate between the different reduction methods as for each reduction method different lines will be kept. The y-axis shows all load cases described earlier in Table 2. A negative difference value appears when the load flow in the reduced grid is lower than in the original grid. In this case, the color gets darker and greener the higher the error. A positive difference appears when the load flow in the reduced grid is higher than in the original grid. In this case, the color gets darker and redder the higher the error. Errors near zero are bright and whitish.

A line having almost the same usage error for each load case indicates a generally poor load flow representation for this line independent from the load case. For all reductions, there are a few single

lines which have high load flow errors in most of the cases. Such errors are more frequent in the PyPSA-reduction than in the ED-reduction. Several lines are close to their original power flows. At reductions of 30% and 20% of the original size, the errors increase and vary not only between different lines but also between different load cases. Overall ED-reduction heat maps are noticeably lighter than the PyPSA-reduction, which means that there are lower errors.

7. Discussion

Energy system models optimize energy production and consumption over all time steps to find a cost minimal system. This means they would structuredly profit or suffer from bad grid representations. Regarding the RMSE as quality indicator for the load flow behavior, the ED-method outperformed the PyPSA-method in all reduction degrees relevant for energy system models. The PyPSA-reduction suffers losses of accuracy due to the possibility of assigning nodes to the same cluster even if they are not connected directly or by other lines inside of their cluster. The replacement of one node per cluster is equivalent to the connection of all cluster's nodes by a lossless copper plate. The electrical flow is usually distorted greatly if non-connected nodes are connected together. This is prevented in the ED-method as only connected nodes can be aggregated together in an iterative way. Nevertheless, for increasing reduction degrees, the impact of the mentioned problem is diminished so that the error discrepancy between the methods decreases.

Although for the ED-method, a reduction to 30% of the original grid nodes results in high maximal expected errors per line with a median of 34%, 82% of the remaining lines have still been correctly detected whether they are overloaded or not. Considering the total line length of the remaining lines, 77% of the original overloaded line length has been detected as overloaded. For the PyPSA-method maximal expected errors per line are even higher with a median of 46%. Nevertheless, the classification accuracy of overloaded line numbers reaches a value of 76% for the remaining lines. In this case 71% of the original overloaded line length has been detected as overloaded when only considering the remaining lines. Although error measures concerning the load flow seem high, a decent detection of overloaded lines could be reached.

It is noticeable that the more the grid is reduced the line length percentage of detected overloaded lines decreases, even when ignoring the lines removed by the grid reduction. The comparison of the DiffMaxAbs value from Section 6.3 indicates a slight underestimation of maximal absolute values in the reduced grids which could explain the lower overload detection accuracy. Additionally, with the intensification of the reduction, power differences between clusters are likelier to lessen. This is due to the increasing probability that aggregating more nodal powers inside of a cluster lead to a more balanced averaged power. This in turn leads to more balanced line flows between clusters and therefore to a less maximal usage rate value per line.

A further issue is the effect of removing lines being overloaded. Several methods try to solve this issue by expanding the line lengths by a constant factor independent from the reduction degree. Table 4 shows that overload detection rates, in terms of line lengths for different reduction degrees, tend to decrease with the intensification of reduction. For energy system analysis a variable factor dependent on the reduction degree might be useful when expanding remaining lines, especially when an estimation of total overloaded line lengths or grid reinforcement costs is desired. When line-specific overload detection is additionally required, an alternate solution might be to detect lines prone to overloads during the grid reduction. An approach to detect such lines can be found in Scheufeld et al. [20]. However, this does not prevent the false overload classification of remaining lines. The presented grid reduction approach is optimized the represent load flows as good as possible by agglomeratively combining nodes with highest admittance in between. This leads to good results regarding quality of load flow representation. However taking additional factors into account would lead to worse results regarding quality of load flow representation. In the case of removed overloaded lines this would mean, that overloaded lines are not removed but the probability to recognize them as overloaded would decline.

Seeking for an indicator evaluating a clustering in terms of potential load flow behavior after the reduction, the rating of modularity considering electrical distance as weights between nodes might be used. Ratings should be used with caution and only clusterings at the same reduction degrees should be compared using it. Looking at the modularity for a specified number of clusters while using the electrical distance as edge weights, higher values might indicate better load flow representations when using the copper plate approach after the grid clustering.

Modeling the electrical grid with PV nodes has the drawback that the voltage levels are fixed at these nodes. This implies an unnecessary high reactive power provision to maintain voltage at the specified level, leading to raised reactive power flows and raised losses. Especially the effect of FACTS and HVDC lines is difficult to correctly account for. AC optimal power flow calculations which could overcome this problem did not converge. The reason for the non-convergence is that load cases were calculated for a future energy system with crucial changes of generation infrastructure. Those changes would normally imply grid reinforcement to maintain a stable electricity system. Since the goal of the paper is to first measure if overloads are detected, including grid reinforcement is not an option. Choosing such load cases is justified by the goal of energy system models, which is mostly to calculate an energy system in the future with new side conditions and therefore strong changes in production and consumption. Hence it is not possible to use the proposed method for stability investigations. Goal of the method is to evaluate if overloads are detected correctly and to classify the results of energy system models regarding this question. After detecting overloads correctly, grid reinforcement measures have to be applied. Stability needs to be investigated for the reinforced grid then.

8. Conclusion

In this paper, a grid reduction method based on electrical distance clustering (ED-reduction) was presented. The method applies an initial clustering of nodes with only a single neighbor, to losslessly reduce the grid to a limited extent. An agglomerative clustering method is then further applied, which uses modularity as a rating measure to further reduce the grid. The ED-reduction method was compared with the reference PyPSA reduction method which does not take the electrical characteristics of clustering into account. Various load flow and overload detection errors were calculated to quantify the comparison.

The presented algorithm considering the grid outperformed the one not considering it in the majority of relevant quality indicators. Especially regarding the RMSE, the ED-reduction method prevailed and therefore contributes to better representations of electrical grids within energy system models. This is important since energy system models would use errors in line usage rates to optimize the energy system where it is not possible.

The detection of overloaded line lengths is an important factor to determine costs for reinforcement measures. In this paper, percentages of detected line overloads and corresponding line lengths could be quantified for several reduction degrees. This investigation may be used to analyze results of energy system models regarding grid reinforcement costs.

In addition to considering the electrical distance, the presented clustering algorithm is able to integrate regional merging and cluster size constraints due to the agglomerative procedure. Furthermore, the number of clusters or alternatively the number of desired regions can be specified to get exactly the grid size desired.

The comparison of the detected overloaded lines and their lengths between the original and reduced grids enables the classification of detected grid reinforcement costs relative to the degree of grid

reduction. The implications of this comparison are essential to an effective energy system analysis. Most importantly, the error that arises as a result of grid reduction can be accounted for in the design and analysis of energy system optimization.

Declaration of Competing Interests

The authors declare that they have no known competing financial interests or personal relationships that could have appeared to influence the work reported in this paper.

CRediT authorship contribution statement

Wolfgang Biener: Conceptualization, Formal analysis, Investigation, Resources, Data curation, Writing - original draft, Writing - review & editing, Visualization, Supervision, Project administration, Funding acquisition. **Klaus René Garcia Rosas:** Methodology, Software, Validation, Formal analysis, Investigation, Data curation, Writing - original draft, Writing - review & editing, Visualization.

Acknowledgments

This research was partially developed within the AutGrid project and has received funding from the German Federal Ministry of Education and Research under grant agreement no. 03EK3557A. Therefore the authors would like to thank the German Federal Ministry of Education.

Appendix A. Line overload classification

Accumulated line lengths for detailled classifications of overload detection and various reduction degrees are displayed in Table A.1.

Table A.1
Line overload detection: accumulated line length in km.

Reduction ▷	ED			PyPSA		
▽ Classification	50%	30%	20%	50%	30%	20%
false negative	1735	2472	2398	2434	3552	4242
false positive	594	873	638	845	1236	839
true negative	8238	5490	4672	8709	7219	6151
true positive	11,314	8369	6679	11,076	8745	6795
NA negative	3306	5774	6828	2584	3682	5148
NA positive	1442	3631	5394	961	2174	3435

References

[1] W. Biener, C. Senkpiel, S. Shammugam, K.R.G. Rosas, M. Linke, O. Eibl, Impact of grid reduction on modelling accuracy of line usage rates, Journal of Physics: Conference Series 977 (1) (2018) 012001. URL http://stacks.iop.org/1742-6596/977/i=1/a=012001
[2] S. Blumsack, P. Hines, M. Patel, C. Barrows, E.C. Sanchez, Defining power network zones from measures of electrical distance, Power & Energy Society General Meeting, 2009. PES'09. IEEE, IEEE, 2009, pp. 1–8.
[3] T. Brown, J. Hörsch, D. Schlachtberger, PyPSA: python for power system analysis, J. Open Res. Softw. 6 (4) (2018), https://doi.org/10.5334/jors.188.
[4] Bundesnetzagentur, Bedarfsermittlung 2017-2030 - Bestätigung des Netzentwicklungsplans Strom für das Zieljahr 2030, Technical Report, Bundesnetzagentur, 2017. URL https://www.netzentwicklungsplan.de/sites/default/files/paragraphs-files/NEP_2030_2017_Bestaetigung.pdf
[5] Bundesnetzagentur, Kraftwerksliste der bundesnetzagentur, 2018. URL https://www.bundesnetzagentur.de/DE/Sachgebiete/ElektrizitaetundGas/Unternehmen_Institutionen/Versorgungssicherheit/Erzeugungskapazitaeten/Kraftwerksliste/kraftwerksliste-node.html.
[6] X. Cheng, T.J. Overbye, Ptdf-based power system equivalents, IEEE Trans. Power Syst. 20 (4) (2005) 1868–1876.
[7] A. Clauset, M.E. Newman, C. Moore, Finding community structure in very large networks, Phys. Rev. E 70 (6) (2004) 066111.
[8] P. Dimo, Nodal Analysis of Power Systems, Abacus Bks, Editura Academiei Republicii Socialisté România, 1975.
[9] J. Egerer, C. Gerbaulet, R. Ihlenburg, F. Kunz, B. Reinhard, C. von Hirschhausen, A. Weber, J. Weibezahn, Electricity sector data for policy-relevant modeling: Data documentation and applications to the german and european electricity markets, Technical Report, DIW, 2014.
[10] ENTSOE, Hourly load, 2018. URL https://www.entsoe.eu/data/power-stats/hourly_load/.
[11] J. Hörsch, T. Brown, The role of spatial scale in joint optimisations of generation and transmission for european highly renewable scenarios, 2017 14th International Conference on the European Energy Market (EEM), (2017), pp. 1–7.
[12] V. Krishnan, J. Ho, B.F. Hobbs, A.L. Liu, J.D. McCalley, M. Shahidehpour, Q.P. Zheng, Co-optimization of electricity transmission and generation resources for planning and policy analysis: review of concepts and modeling approaches, Energy Syst. 7 (2) (2016) 297–332, https://doi.org/10.1007/s12667-015-0158-4.
[13] V. Krishnan, J.D. McCalley, S. Lemos, J. Bushnell, Nation-wide transmission overlay design and benefits assessment for the U.S. Energy Policy 56 (2013) 221–232, https://doi.org/10.1016/j.enpol.2012.12.051.
[14] M. Kurzidem, Analysis of Flow-based Market Coupling in Oligopolistic Power Markets, ETH Zürich, 2010 Ph.D. thesis.
[15] P. Lopion, P. Markewitz, M. Robinius, D. Stolten, A review of current challenges and trends in energy systems modeling, Renew. Sustain. Energy Rev. 96 (2018) 156–166, https://doi.org/10.1016/j.rser.2018.07.045.
[16] J. McCalley, V. Krishnan, K. Gkritza, R. Brown, D. Mejia-Giraldo, Planning for the long haul: investment strategies for national energy and transportation infrastructures, IEEE Power Energy Mag. 11 (5) (2013) 24–35, https://doi.org/10.1109/MPE.2013.2268712.
[17] H.-K. Ringkjøb, P.M. Haugan, I.M. Solbrekke, A review of modelling tools for energy and electricity systems with large shares of variable renewables, Renew. Sustain. Energy Rev. 96 (2018) 440–459, https://doi.org/10.1016/j.rser.2018.08.002.
[18] R.J. Sánchez-García, M. Fennelly, S. Norris, N. Wright, G. Niblo, J. Brodzki, J.W. Bialek, Hierarchical spectral clustering of power grids, IEEE Trans. Power Syst. 29 (5) (2014) 2229–2237.
[19] E.E. Sauma, S.S. Oren, Proactive planning and valuation of transmission investments in restructured electricity markets, J. Regul. Econ. 30 (3) (2006) 358–387, https://doi.org/10.1007/s11149-006-9012-x.
[20] O. Scheufeld, L. Kalisch, A. Moormann, S. Krahl, A. Moser, Assessment of the structural characteristics of electrical transmission systems using a graph theoretic measure, International ETG Congress 2017, (2017), pp. 1–6.
[21] C. Senkpiel, W. Biener, S. Shammugam, S. Längle, Evaluation of load flow and grid expansion in a unit-commitment and expansion optimization model scigrid international conference on power grid modelling, Journal of Physics: Conference Series 977 (1) (2018) 012008. URL http://stacks.iop.org/1742-6596/977/i=1/a=012008
[22] C. Senkpiel, S. Shammugam, W. Biener, N.S. Hussein, C. Kost, N. Kreifels, W. Hauser, Concept of evaluating chances and risks of grid autarky, European Energy Market (EEM), 2016 13th International Conference on the, IEEE, 2016, pp. 1–5.
[23] B. Stott, O. Alsac, Fast decoupled load flow, IEEE Trans. Power Appar. Syst. PAS-93 (3) (1974) 859–869.
[24] H.G. Svendsen, Grid model reduction for large scale renewable energy integration analyses, Energy Procedia 80 (2015) 349–356.
[25] H. Temraz, M. Salama, V. Quintana, Application of partitioning techniques for decomposing large-scale electric power networks, Int. J. Electr. Power Energy Syst. 16 (5) (1994) 301–309.
[26] J.B. Ward, Equivalent circuits for power-flow studies, Electr. Eng. 68 (9) (1949) 794.
[27] L. Welder, D. Ryberg, L. Kotzur, T. Grube, M. Robinius, D. Stolten, Spatio-temporal optimization of a future energy system for power-to-hydrogen applications in germany, Energy 158 (2018) 1130–1149, https://doi.org/10.1016/j.energy.2018.05.059.
[28] F. Wiese, R. Bramstoft, H. Koduvere, A.P. Alonso, O. Balyk, J.G. Kirkerud, Åsa Grytli Tveten, T.F. Bolkesjø, M. Münster, H. Ravn, Balmorel open source energy system model, Energy Strategy Rev. 20 (2018) 26–34, https://doi.org/10.1016/j.esr.2018.01.003.